Thermal Stratification Performance of a Packed Bed Latent Heat Storage System during Charging

Ashmore Mawire[1], *Katlego* Lentswe[1], *Robert* Lugolole[2], *Denis* Okello[2], and *Karidewa* Nyeinga[2]

[1]Department of Physics and Electronics, Private Bag, X2046, Mmabatho 2745, South Africa
[2]Department of Physics, Makerere University, P.O. Box 7062, Kampala, Uganda

Abstract. Experimental thermal stratification evaluation of a packed bed latent heat storage is done during charging cycles. The packed bed latent heat storage system consists of adipic acid encapsulated in aluminum spheres. Sunflower oil is used as the heat transfer fluid during charging cycles. Stratification number profiles are used to evaluate thermal stratification in the storage system. Charging experiments are carried out with three different flow-rates (4 ml/s, 8 ml/s and 12 ml/s). Charging experiments are also done using the same flow-rate (8 ml/s) with three different set heater temperatures (220 ^{o}C, 240 ^{o}C and 260 ^{o}C). The lowest charging flow-rate (4 ml/s) shows the best variation of the stratification number profile since it shows the least drop from the peak value and the shortest charging interval. Different set heater temperatures show almost identical stratification number profiles. The effect of the charging flow-rate is more significant than the effect of the charging set heater temperature when evaluating thermal stratification for this particular system.

1 Introduction

The charging efficiency of thermal energy storage (TES) tanks is enhanced by thermal stratification. Stratification in the storage tank results from buoyancy effects cause by density differences in the storage. The hotter fluid rises to the top and the colder fluid falls to the bottom. A thermal gradient thus exists between the top and the bottom of the storage tank. The region between these two regions in liquid based TES systems known as thermocline should be kept at a minimal possible thickness for increased efficiency of the systems.

Studies on thermal stratification have been predominantly on water storage for domestic hot water systems [1-5]. For higher medium temperature applications (100 ^{o}C to 300 ^{o}C), the hot water storage tank is not suitable since water has to be pressurized for these applications making storage tank design complicated. Thermal oil storage tanks can be used since oil vaporizes at higher temperatures than this stipulated range. Limited recent studies have been reported on thermal performance and stratification for medium temperature applications using thermal oils [6-10], hence it necessary to carry out this study to understand the efficiency of these systems.

Latent heat storage has advantages of a larger thermal storage density and nearly iso-thermal behaviour during the storage and release of energy as compared to sensible heat storage. There have been also very few studies on oil based latent heat packed TES systems for medium temperatures [11-13]. Adipic acid has recently been proposed as a suitable PCM for medium temperature applications [14-15], but no study has ever been done using it in a packed bed storage configuration. Sunflower oil is selected as the HTF since it is cheap, food grade, and readily available, non-toxic and possesses characteristics comparable to other commercial HTFs as previously investigated in [16]. The potential application of this storage system is in solar cooking. The storage system can be used for storage of solar thermal energy which can be used at night or during cloudy periods when the sun is not available. The aim of this paper is to evaluate the charging stratification performance a Sunflower oil based packed bed latent heat storage system using adipic acid encapsulated in aluminum spheres. The objectives are to evaluate the stratification performance using different set heater charging temperatures and also using different charging flow-rates.

2 Experimental methods

2.1 Encapsulated phase change materical (PCM) spheres

Adipic acid was poured into forty spherical aluminum capsules with diameters of 0.05 m and wall thicknesses of 0.001 m. The capsules were manufactured as hollow spheres with an opening at the top to allow for pouring of PCM. The volume of the PCM in the capsules was about 80 % of the total internal volume of the capsule to allow for thermal expansion. The volume to be poured into the capsule was measured very carefully with a small

measuring cylinder. Adipic acid was in a small crystalline form such that it could be poured easily in its solid form into the capsules. After pouring of adipic acid, four capsules had K-thermocouples fixed onto them to measure the PCM temperature. These thermocouples which extended into the centre of the spheres were fastened on the top of the spheres. The thermocouples acted both as sealing mechanisms and also as temperature monitoring devices. The rest of the PCM capsules were sealed with screw caps. Fig. 1 shows a PCM capsule with a screw cap and one with a thermocouple screw cap.

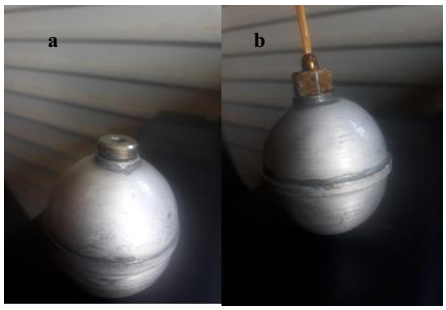

Fig. 1. (a) Aluminum PCM capsule with screw cap. (b) Aluminum capsule with thermocouple screw cap.

Thermo-physical properties of adipic acid obtained from open literature are shown in Table 1. The melting temperature of adipic acid is reported to be around 152 ^{o}C.

Table 1. Thermo-physical properties of adipic acid.

Property	Value
Melting Temperature (^{o}C)	150-152 [15]
Specific Heat Capacity (kJ/kgK)	1.59 (20 ^{o}C), 2.26 (150 ^{o}C] [14]
Phase change enthalpy (kJ/kg)	213–260 [15]
Density(kg/m^{3})	1360 (20 ^{o}C), 1093 (163 ^{o}C) [19]
Thermal conductivity (W/mK)	0.142-0.162 [18]
Average mass of PCM in the capsules (g)	~40

2.2 Experimental setup and procedure

The experimental setup of the TES system is shown in the schematic diagram of Fig. 2.

Forty spherical PCM capsules were inserted into the storage and the top level capsules were at level A below the tank inlet port. The void between the capsules was filled with Sunflower oil up to level A. The electric unit (g) consisted of two copper spiral coils (power rating: 220V, 900 W each) to heat up the circulating oil and it was controlled by a temperature controller. The TZN4S temperature controller (h) (display accuracy: ±0.3 %) was used to set and control the required maximum temperature. An insulated stainless steel cylindrical storage tank (a) with a diameter of 0.3 m and a height of 0.54 m was used. K-type thermocouples (accuracy: ± 1 %) were placed at radial distances of 0.013 m, 0.038 m and 0.064 m to measure temperature at each axial level of the storage tank (Levels A-D). Four PCM capsules with thermocouples were placed centrally at Levels A-D, to monitor the PCM temperature at each level. The thermocouples were calibrated to an accuracy of around ±2 ^{o}C. The storage tank was filled with 4 litres of refined Sunflower oil during the experiments. A magnetic-drive pump (b) was used to circulate the Sunflower oil through the heating unit while a VLT Micro drive (c) (maximum error: 0.8% of full scale) was used to control the frequency of the pump so as to set a desired flow-rate. A flow meter (maximum operating temperature: 120 ^{o}C) (f) was used to measure the flow rate of the TES system every 10 s and a heat exchanger (e) was connected directly to the flow meter to cool it down so as not to exceed its maximum operating temperature. An HP 34970 data acquisition unit (j) was connected to the thermocouples and it was used to convert analogue signals to digital signals. A personal computer (i) was used to monitor the temperature profile of the TES system and the PCMs and it recorded data every 10 s.

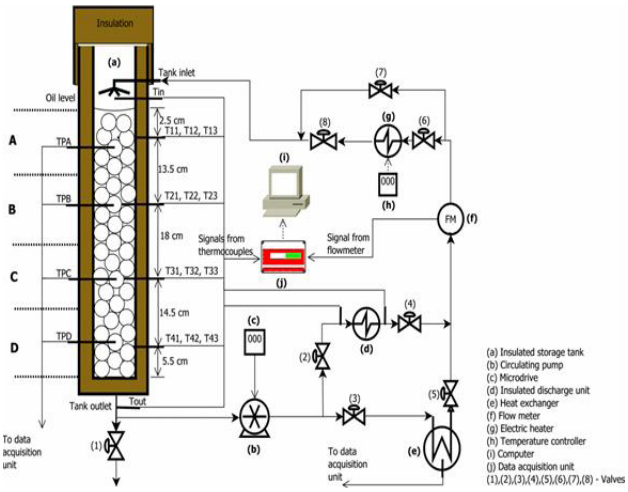

Fig. 2. Schematic diagram of experimental setup.

During the charging cycles valves (1), (2), (4) and (7) were closed while valves (3), (5), (6) and (8) were opened. Charging of the storage system was terminated when the bottom temperature of the storage tank (TD) was around 170 ^{o}C. Charging experiments were performed with flow-rates of 4 ml/s, 8 ml/s and 12 ml/s respectively at a set temperature of 260 ^{o}C to investigate the effect of the flow-rate. To investigate on the effect of the set temperature, charging experiments were performed at a flow-rate of 8 ml/s with heater set temperatures of 220 ^{o}C, 240 ^{o}C and 260 ^{o}C respectively. Charging experiments were performed from the top to the bottom of the storage tank.

3 Thermal analysis

The temperature at each level is the average of the measured radial temperatures. The stratification number is given by the ratio of the mean temperature gradients at any time to the maximum mean temperature gradient during the charging cycle [17]. The equation is expressed as:

$$Str = \frac{\left(\frac{\partial T}{\partial z}\right)_t}{\left(\frac{\partial T}{\partial z}\right)_{max}} \quad (1)$$

where T is the average temperature at each axial level and z is axial position. The thermal gradient is expressed as;

$$\frac{\partial T}{\partial z} = \frac{1}{n-1}\left[\sum_{1}^{n-1}\left(\frac{T_{n+1} - T_n}{\Delta Z_n}\right)\right] = \frac{1}{3}\left[\sum_{1}^{3}\left(\frac{T_{n+1} - T_n}{\Delta Z_n}\right)\right] \quad (2)$$

4 Results and discussion

4.1 Effect of flow-rate

Fluid temperatures at the four levels of the storage tank with different flow-rates at a set heater charging temperature of 260 °C are shown in Fig. 3.

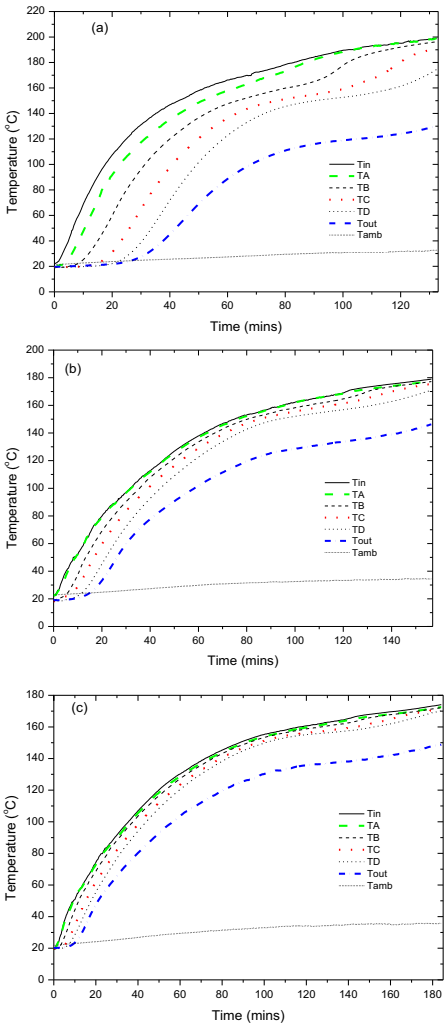

Fig. 3. Fluid temperatures at a set heater temperature of 260 °C with charging flow-rates of (a) 4 ml/s (b) 8 ml/s and (c) 12 ml/s.

An increase in the flow-rate increases the charging time. The rate of temperature rise is faster with an increase in the flow-rate which results in a faster rate of heat loss at higher flow-rates. These heat losses occurring faster with higher flow-rates result in attaining the bottom limiting charging temperature at a later time. Phase change transition commences from the top and occurs later at the bottom of the storage tank since the tank is charged from the top to the bottom. More pronounced thermal stratification and phase change transition around 150 °C is seen with the lowest flow-rate suggesting that charging at the lowest flow-rate is more beneficial for maintaining a higher degree of stratification. The phase change transition occurs earlier and is more pronounced with the lowest flow-rate. For instance, the phase change transition at the bottom of the storage tank starts at around 80 mins for 4 ml/s whereas for flow-rates of 8 ml/s and 12 ml/s it starts at around 100 mins and 110 mins respectively. The lowest charging flow-rate (4 ml/s) also results in higher temperatures at the top of the storage tank at the end of charging.

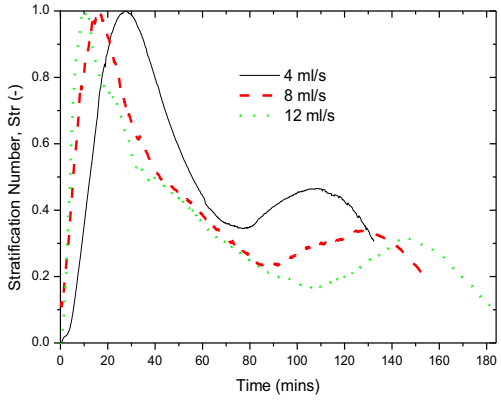

Fig. 4. Stratification number profiles at a set heater temperature of 260 °C with different charging flow-rates.

Stratification number profiles using the three flow-rates are shown in Fig. 4. The fastest rise to the peak stratification number is seen with the highest flow-rate due to the fastest rate of heat transfer. After this initial rise, the stratification number profiles begin to drop due the more pronounced and significant temperature rise at the bottom of the storage tank. The best stratification distribution is seen with the lowest flow-rate, although it has the slowest rise to the peak value. The drop of the stratification number is less with the lowest flow-rate as compared to the other flow-rates. During the phase change process, the thermal gradients of the fluid temperatures tend to decrease and flatten. This behaviour is depicted by the stratification number profiles. For the lowest flow-rate, this behaviour occurs earlier between 60 to 80 mins. For 8 ml/s and 12 ml/s it occurs later between 80 to 100 mins and between 100 to 120 mins respectively. The stratification number values for the lowest flow-rate are higher than the other flow-rates after the peak values making the best charging flow-rate. It is also important to note that there are additional secondary maxima after the peak values due to the rise in the thermal gradients of the fluid temperatures after the phase change process. The secondary peak value is higher for the lowest flow-rate and it occurs earlier at around 110 mins. Additional stratification number drops

after the secondary peaks can also be explained by the drops in the thermal gradients of the fluid temperatures.

4.2 Effect of set heater charging temperature

Fluid temperature profiles with different set heater temperatures are presented in Fig. 5.

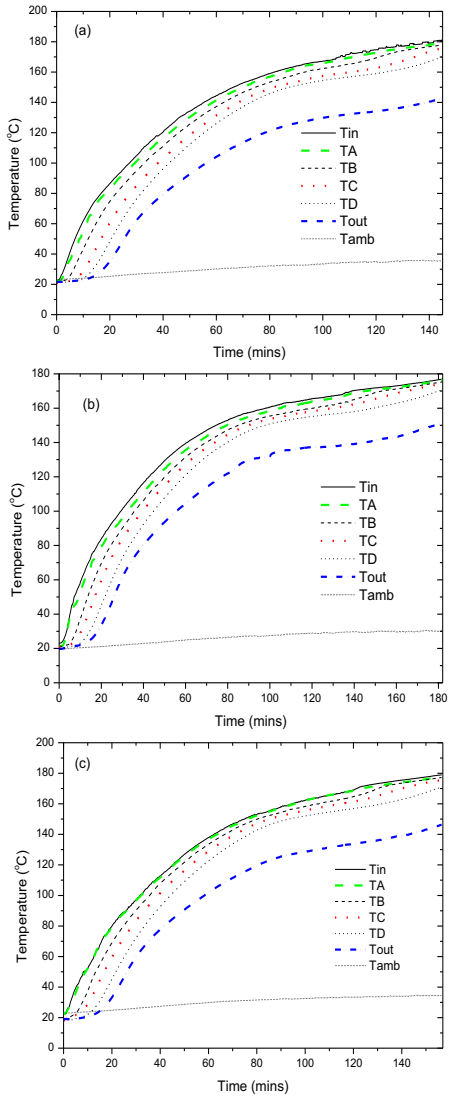

Fig. 5. Fluid temperatures at a charging flow-rate of 8 ml/s with set heater temperatures of (a) 220 °C (b) 240 °C and (c) 260 °C.

Increasing the set heater temperature seems to increase the charging time possibly due to increased heat losses associated with higher set heater temperatures. The charging time for the 240 °C (~180 mins)case is longer than that for the 260 °C (~ 156 mins) case possibly because of the lower ambient temperatures associated with 240 °C . The storage tank was charged for a longer time with 240 °C because the bottom limiting storage tank temperature was reached at a later time due to the higher corresponding heat losses at lower ambient temperature conditions. The temperature rise with the lowest set temperature (220 °C) is slightly higher at the top of the storage but it seems comparable at the bottom of the storage tank. As an illustrative example, the inlet temperature is around 160 °C at 80 mins for 220 °C whereas it is around 150 °C for 240 °C and 260 °C. The outlet temperatures are comparable and they are around 120 °C at 80 mins for the three set temperatures. Different set temperatures only result in a marginal variation of the phase transition times as compared to the flow-rate effect depicted in Fig. 3. The degree of stratification during the charging process seems to be comparable for the three set temperatures.

Stratification number profiles for different set heater temperatures with the same flow-rate of 8 ml/s are shown in Fig. 6. The rate of rise of the stratification number to the peak value is almost identical and the peak values occur at almost the same time of around 15 mins. The drops from the peak values are almost identical up to around 80 mins. These drops are due the bottom level temperatures rising appreciably from 20 to 80 mins thus reducing the axial thermal gradients. The lowest set temperature shows slightly higher values of the stratification from 80 mins to 140 mins, however, the phase change transition flattening occurs at the same time as the 260 °C case. Due to higher heat losses, the phase change flattening and the secondary peak for the 240 °C case occurs later. In general, the stratification profiles for the three set temperatures are comparable and only slightly better performance is seen with the lowest set temperature. The stratification number profile is more dependent on the flow-rate than on the set heater charging temperature. A lower flow-rate induces the phase change process more significantly and thermal stratification is more pronounced. The charging time is also reduced with the lower flow-rate for this particular system.

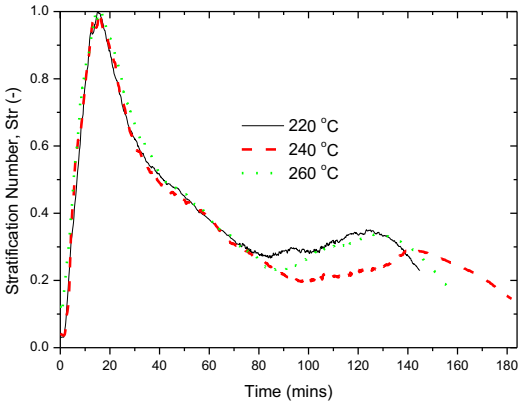

Fig. 6. Stratification number profiles at different set heater temperatures with a charging flow-rate of 8 ml/s.

4 Conclusion

An experimental setup to evaluate thermal stratification in a packed bed latent heat storage during charging cycles was designed. The packed bed latent heat storage system consisted of adipic acid encapsulated in aluminum spheres. Sunflower oil was used as the heat transfer fluid during charging cycles. Stratification number profiles were used to evaluate thermal stratification in the storage tank. Charging experiments were carried out with three different flow-rates (4 ml/s, 8 ml/s and 12 ml/s). Charging experiments were also done using the same

flow-rate (8 ml/s) with three different set heater temperatures (220 ^{o}C, 240 ^{o}C, 260 ^{o}C). The lowest charging flow-rate (4 ml/s) showed the best variation in the stratification number profile since it showed the least drop from the peak value and the shortest charging interval. Different set heater temperatures showed almost identical stratification number profiles during charging. The effect of the charging flow-rate was more significant than the effect of the charging set heater temperature when evaluating thermal stratification for this particular system.

Acknowledgment

The authors wish to acknowledge NRF South Africa (Grant No: UGAG160513164998 and IFRR-Grant number: 90638) for making funds available to carry out this research.

References

1. Kong L, Zhu N. CFD simulations of thermal stratification heat storage water tank with an inside cylinder with openings (2017). Procedia Engineering 146; 394-99.
2. Wang Z, Zhang H, Dou B, Huang H, Wu W, Wang. Experimental and numerical research of thermal stratification with a novel inlet in a dynamic hot water storage tank (2017). Renewable Energy 111; 353-71.
3. Bouhal T, Fertahi S, Agrouaz Y, El Rhafiki T, Kousksou T, Jamil A. Numerical modeling and optimization of thermal stratification in solar hot water storage tanks for domestic applications: CFD study (2017). Solar Energy 157; 441-55.
4. García-Marí E, Gasque M, Gutiérrez-Colomer RP, Ibáñez F, González-Altozano P. A new inlet device that enhances thermal stratification during charging in a hot water storage tank (2013). Applied Thermal Engineering 61; 663-69.
5. Jordan U, Furbo S. Thermal stratification in small solar domestic storage tanks caused by draw-offs (2005). Solar Energy 78; 291-300
6. Mawire A, Taole S, Phori A. Performance comparison of thermal energy storage oils for solar cookers during charging (2014). Applied Thermal Engineering 73;1321-29.
7. Mawire A, Taole S. A comparison of experimental thermal stratification parameters for an oil/pebble-bed thermal energy storage (TES) system during charging (2011). Applied Energy 88; 4766-78.
8. Bruch A, Fourmigue´ JF, Couturier R. Experimental and numerical investigation of a pilot-scale thermal oil packed bed thermal storage system for CSP power plant (2014). Solar Energy 105; 116-25.
9. Bruch A, Molina S, Esence T, Fourmigue´ JF, Couturier R. Experimental investigation of cycling behaviour of pilot-scale thermal oil packed-bed thermal storage system (2017). Renewable Energy 103: 277-85.
10. Erregueragui Z, Boutammachte N, Bouatem A, Merroun O, Zemmouri E. Packed-bed Thermal Energy Storage Analysis: Quartzite and Palm-Oil Performance (2016). Energy Procedia 99; 370-79.
11. Shobo AB, Mawire A. Experimental comparison of the thermal performances of acetanilide, meso-erythritol and an In-Sn alloy in similar spherical capsules (2017). Applied Thermal Engineering 124; 871-82.
12. Shobo AB, Mawire A, Okello D. Experimental thermal stratification comparison of two storage systems (2017) Energy Procedia 142; 3295-3300.
13. Kumaresan G, Vigneswaran VS, Esakkimuthu S, Velraj R. Performance assessment of a solar domestic cooking unit integrated with thermal energy storage system (2016). Journal of Energy Storage 6; 70-79.
14. Haillot D, Bauer T, Kröner U, Tamme R. Thermal analysis of phase change materials in the temperature range 120–150 °C. (2011). Thermochimica Acta 513; 49–59.
15. Gasia J, Martin M, Solé A, Barreneche C, Cabeza LF. Phase Change Material Selection for Thermal Processes Working under Partial Load Operating Conditions in the Temperature Range between 120 and 200 ^{o}C (2017). Applied Sciences17; 772 (1–14).
16. Mawire A, Performance of Sunflower Oil as a sensible heat storage medium for domestic applications (2016). Journal of Energy Storage; 5:1–9.
17. Fernández-Seara J, Uhía FJ, Sieres J. Experimental analysis of a domestic electric hot water storage tank. Part II: dynamic mode of operation (2007). Applied Thermal Engineering 27; 137-44..
18. Adipure Datasheet (2018). http://adi-pure.invista.com/e-trolley/page_11546/index.html ,website accessed March 20018
19. Chemistry Dashboard (2018)mhttps://comptox.epa.gov/dashboard/dsstoxdb/results?search=Adipic+acid-2%2C2%2C5%2C5-d4 , website accessed March 2018